A Journal of the Gesellschaft Deutscher Chemiker

Angewandte International Edition GDCh Chemie

www.angewandte.org

Accepted Article

Title: Information Coding in Reconfigurable DNA Origami Domino Array

Authors: Sisi Fan, Dongfang Wang, Jin Cheng, Yan Liu, Tao Luo, Daxiang Cui, Yonggang Ke, and Jie Song

To be cited as: *Angew. Chem. Int. Ed.* 10.1002/anie.202003823

Link to VoR: https://doi.org/10.1002/anie.202003823

WILEY-VCH

10.1002/anie.202003823

WILEY-VCH

RESEARCH ARTICLE

Information Coding in Reconfigurable DNA Origami Domino Array

Sisi Fan[a], Dongfang Wang[a], Jin Cheng[a], Yan Liu[a], Tao Luo[a], Daxiang Cui[a], Yonggang Ke[b], Jie Song[a][c]*

[a] S.S. Fan, Dr. D.F Wang, J. Cheng, Y. Liu, T. Luo, Prof. D.X. Cui, Prof. J. Song*
Institute of Nano Biomedicine and Engineering,
Department of Instrument Science and Engineering,
School of Electronic Information and Electrical Engineering,
Shanghai Jiao Tong University, Shanghai 200240, China.
*E-mail: sjie@sjtu.edu.cn

[b] Prof. Y.G. Ke,
Wallace H. Coulter Department of Biomedical Engineering,
Georgia Institute of Technology and Emory University,
30322, Atlanta, GA, USA

[c] Prof. J. Song
Institute of Cancer and Basic Medicine (IBMC), Chinese Academy of Sciences;
The Cancer Hospital of the University of Chinese Academy of Sciences, Hangzhou, Zhejiang 310022, China.

Abstract: DNA nanostructures with programmable nanoscale patterns has been achieved in the past decades, and molecular information coding (MIC) on those designed nanostructures has gained increasing attention for information security. However, exerting steganography and cryptography synchronously on DNA nanostructures still remains a challenge to guarantee more security approach for MIC. Here, we demonstrated MIC in a reconfigurable DNA origami domino array (DODA), which can reconfigure intrinsic patterns but keep the DODA outline the same for steganography. When a set of keys (DNA strands) are added, the cryptographic data (e.g. Numbers “0 - 9”) can be translated into visible patterns within DODA. More complex cryptography with ASCII nanocodes definition within programmable 6×6 lattice is demonstrated to ensure the versatility of MIC in the DODA. Furthermore, a further anti-counterfeiting approach based on conformational transformation mediated toehold strand displacement reaction is designed to protect MIC from decoding and falsification, presenting a unique high-security level approach for information processing.

Introduction

Information coding, which mainly involves in information storage and security, is of great importance in economic and military fields as well as in our daily life. The key requirements of MIC technologies are difficulty in duplication, less randomness, high data storage density, and uniqueness of the data verification. With advantages of programmable position and addressable pixel, structural DNA nanotechnology has been used to assemble diverse components for DNA nanostructure-based MIC[1].

DNA origami[2], as one of popular structural DNA nanotechnology, is specially suitable in MIC. On one hand, the synthesis of DNA origami is actually an MIC process by folding the long DNA single scaffold with hundreds of short DNA strands (called staples) to form pre-designed shapes. Those specific shapes with MIC could not be duplicated only if the right staple library keys present. On another hand, apart from the bare DNA origami, each single staple can be modified with guest molecules such as Au nanoparticles[3], proteins[4], organic dyes[5], and other materials[6]. The modification makes DNA origami powerful in the addressability of specific sites on the structure with sub-nanometer precision and accuracy, allowing the additional secured information to be tailored into the DNA origami without any randomness. Benefiting from the advantages of DNA origami, MIC, e.g. nano-encrypted Morse code[4], visible patterns information in static DNA origami by well-defined 2D AuNPs networks, digits[5b] and character[7] with high spatial resolution down to ~5 nm by DNA-PAINT have been achieved. More concretely, the process of MIC in static DNA origami is beneficial by the modification of selected staple strands (we call them as active handles). The coded information can be revealed by simply binding the guest molecules to active DNA handles. Consequently, the outputs are provided in a straightforward predictable manner, and the coded information can be read directly[8].

To enhance the MIC security level, different functional DNA origami[9] presenting changeability properties, such as DNA origami nanoactuator[10], DNA walkers[11], and reconfigurable structures[12], have been applied. In this way, the pre-integrated information can be rearranged and displayed along with the dynamic behaviors of these mediums, and it is beneficial to information security. However, the majority of dynamic DNA origami is designed to contain mainly static template joined by a few small dynamic units to take only a single step or a few steps of transformation by using strand-displacement reactions[13] or environmental factors such as pH[14], light[15], electricity[16], magnetic field[17], etc. The dynamic behaviors of large-scale, complex DNA structures templates are still limited. And further advances in the ability to control the movement of DNA origami structures would open up new windows for information security. Thus, it is desirable to develop such dynamic DNA origami as information encoding substrate to store and encode important information for advanced information security.

In this work, a novel MIC strategy based on our group’s previous reconfigurable DODA[18] was reported. The constructed DODA that transformed from one array conformation to another after adding a unique set of keys was especially a suitable candidate for advanced information security. The information was firstly stored and coded in the “Before” conformational DODA, after adding a set of decoding keys (DNA strands), the locations of pre-designed information were rearranged in the “After” conformational DODA, decoding the encoded information. Illustratively, the visual patterns with number “0 - 9” and more complex ASCII barcodes “particular years” and “NO PAINS NO GAINS” messages were successfully presented in the reconfigurable DODA with high security performance. In addition,

10.1002/anie.202003823
WILEY-VCH

RESEARCH ARTICLE

a further anti-counterfeiting approach based on conformational transformation mediated toehold strand displacement reaction was designed to enhance the MIC complexity, and the anti-counterfeiting patterns “S-J-T-U” were successfully decoded with two sets of DNA strands as keys. This elegant DODA is capable of bearing abound information and providing outputs not in a straightforward predictable manner, and the coded information cannot be read until after the specially designed decoding process, overcoming the key difficulties in MIC technologies.

Results and Discussion

Scheme 1 showed the specific advantages of MIC in reconfigurable DODA compared with that in the static DNA origami. In our group’s previous study[18], we reported the assembly and controlled, multistep, long-range transformation dynamic behaviors of reconfigurable DODA. As described therein, the DODA was assembled by interconnected modular dynamic units (anti-junctions) that could transfer their structural information to neighbors. And the dynamic behaviors may enable a range of applications such as information security. Based on it, we selected a 6×6 lattice, which also kept similar size and shape after transformation, for MIC (Scheme 1A). To clearly show the specific advantages of MIC in reconfigurable DODA compared with in the static DNA origami, we took the pattern of digit “4” as an example. As shown in Scheme 1B, readout of the coded digit “4” was accomplished by binding the small molecule to selected staple strands in the static DNA origami. While in the reconfigurable DODA, the coded digit “4” was decoded by taking advantage of the nanostructure transformation as a key (Scheme 1C). The controlled dynamic behavior of DODA enabled a more layer for information protection, providing a novel thought for information security. To further enhance the MIC complexity, an anti-counterfeiting MIC was designed. The coded information could only be decoded with the two keys of conformational transformation and the activation of the inhibited DNA assembly simultaneously. Note that the activation of the inhibited DNA assembly could only be realized after the conformation transformation of DODA (Scheme 1D)

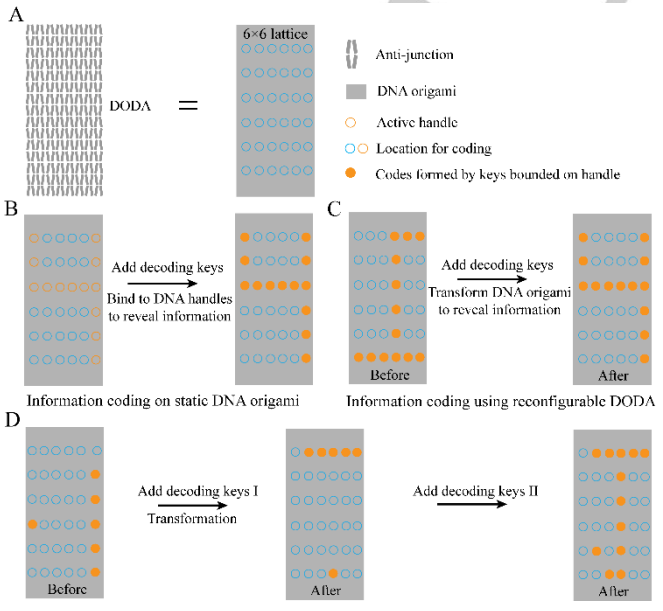

Scheme 1. Schematic of MIC process in reconfigurable DODA. (A) The encoding substrate reconfigurable DODA was constructed by the dynamic DNA unit called “anti-junctions”[19]. To realize the MIC process, we selected a 6×6 lattice to carry information. (B) The process of MIC on static DNA origami. The coded information was revealed by binding guest molecules such as Au nanoparticles, proteins, organic dyes, and other materials to pre-designed DNA handles. (C) The process of MIC using reconfigurable DODA. Biotinylated DNA strands were incorporated into the array at selected locations to store coded information. After adding a set of decoding keys (DNA strands), the locations of biotinylated DNA strands were rearranged in the “After” conformational DODA, revealing the hidden information. (D) The anti-counterfeiting patterns “S-J-T-U” were only decoded with two sets of keys --- one for the conformational transformation and the other for activation of the inhibited information. Scale bar, 100 nm.

To realize the MIC process, it was prior to prepare the encoding substrate reconfigurable DODA. As shown in Figure 1A and Figure S1, different from the static DNA origami reported before[2], the self-assembled DODA was constructed by the dynamic DNA units called “anti-junctions” (the gray ones) [19],which could switch between two stable conformations - “Before” and “After” by adding the green trigger DNA strands. The transformation yield was high (＞93.2%, Figure S2 and Table S1). And such high transformation yield ensured the reliable decoding process. The native agarose gel electrophoresis (Figure 1B) indicated the successful formation of the two conformations of the DODA. And the same mobility of the two conformations bands could also indicate the size of them were similar to some extent. Confirmatively, the AFM images depicted in Figure S3 further revealed the “Before” and “After” conformational DODA were both in rectangular shape with approximately the same size. Consequently, it was difficult for the attacker to recognize them clearly unless they had the correct keys. In this way, we could also regard the encoding substrate DODA as a hiding medium. While in order to identify the two different conformational DODAs much more easily, the scaffolded loops (the orange curves in Figure 1A) were served as the mark. The AFM images (Figure 1C-D) clearly showed the changes between the two conformations of the DODA with the aid of $NiCl_2$. Based on the results of the transformation, it clearly demonstrated that reconfigurable DODA could keep consistency in shape and size, while the structural information changed totally. Afterwards, we explored the designed reconfigurable DODA as information hiding medium, which could be advantageous in steganography and cryptography for advanced MIC.

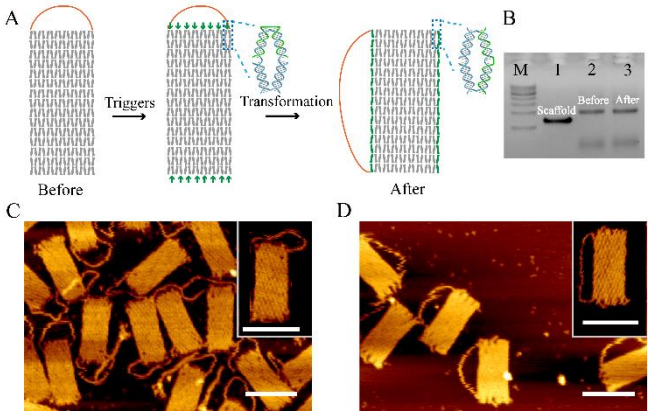

Figure 1. Conformation Transformation of DODA. (A) Schematic of DODA transforms from the “Before” to “After” conformation after addition of trigger strands. (B) The 1% agarose gel analysis of the two conformations of the DODA.

10.1002/anie.202003823
WILEY-VCH

Lane M: 1kb DNA marker. Lane 1: scaffold P7560. Lane 2: "Before" conformation. Lane 3: "After" conformation. (C) AFM picture of the "Before" conformational DODA. (D) AFM picture of the "After" conformational DODA. Note that the AFM pictures were obtained with the aid of $NiCl_2$. Scale bars, 100 nm.

To demonstrate the potential application of the designed reconfigurable DODA in MIC, we firstly created simple patterns, which allowed the visualization of a successful coding and decoding process by the transformation. Patterns, as one kind of expressions of information, could be created associating with DNA origami by various ways. One alternative way reported by Rothemund[2] was to bind the DNA scaffold and fold it into arbitrary shapes, then staple strands decorated the shapes with arbitrary patterns. Another popular way was to mix appropriate modified strands on the DNA origami. In principle, a variety of DNA modifications such as biotin, fluorophores, dumbbell hairpins and so on could serve as labels. Here we took advantage of simple streptavidin (STV)-biotin interaction (Figure S4) to create informational patterns in the reconfigurable DODA. In AFM images, STV attached biotin-staples gave greater height contrast (4 nm above the mica), and each protrusion observed on the DODA surface was a given location representing a piece of meaningful information.

Based the above results that the two different conformational DODA kept consistency in shape and size, the DODA could be applied as the hiding medium in steganography. More specifically, as shown in Figure 2A, in the MIC process, firstly, the sender, who held the proper scaffold strand and information carried staple strands, encoded the plaintext into a braille-like spot pattern cipher in the "Before" conformational DODA, forming a camouflage medium. Afterwards, the camouflage medium (encoded "Before" DODA) was sent to the receiver, and the receiver started decoding the information via two steps: 1) adding the indictor STV to reveal the patterns. Note that the invisible biotinylated positions introduced additional protection by steganography. 2) adding the trigger DNA strands, transforming the conformation of DODA from "Before" to "After". As a result, the transformation allowed the rearrangement of the information locations, thus decoded the information. Notably, benefiting from the consistency in shape and size of the two different conformational DODA, the transformational decoding process was completely confidential without raising any suspicions. We took the digit "4" as an example to present the details of the coding and decoding patterns in DODA (Figure 2B). Initially, we selected a 6×6 lattice, which also kept similar size and shape after transformation, for creating patterns (Figure S5, red ones). The specific biotin-modified staple strands that constituted digit "4" were selected from the 36 biotin-modified staple strands (Figure S10 and Table S3), while the others were still the original staple strands. Then the biotinylated DNA strands that coded pattern of digit "4" were incorporated into the array at selected locations after annealing process. After adding the indicator STV, an illegible digit "4" in "Before" DODA lighted up. Afterwards, after adding the decoding keys (green triggers) to change the conformation to "After", the locations of biotinylated DNA strands coding digit "4" changed and thus decoded the digit "4", making it much more legible. Figure 2B clearly illustrated the specifically dynamic transformation process. The 3D images of the pattern digit "4" (insets in Figure 2C and D) showed the changes between "Before" and "After" conformations. As for a further application in MIC for reliable transmission, it was crucial to calculate efficiency of the STV attachment in given sites. As STV attachment events occurred with an equal and independent probability for each biotin sites, the attachment histograms were expected to follow a binomial distribution, P(m), given by

$$\mathrm{P(m)} = \frac{n!}{m!(n-m)} p^m (1-p)^{n-m} \qquad (1)^{[6a]}$$

where n was the given number of available biotin binding sites per digit and m was the number of actual attached STV. The average attachment probability, p, was given by

$$p = \frac{\sum attached\ STV}{\sum available\ sites} \qquad (2)^{[6a]}$$

where the numerator was the total number of attached STV, and the denominator was the total number of available attachment sites. Firstly, the average attachment probabilities were calculated using *eq 2* from the histogram data to be 0.87 for "Before" conformation and 0.95 for "After" conformation. The solid lines in Figure 2C-D plotted the calculated binomial distribution of *eq 1* for each case, and the binomial distribution in "After" conformation (Figure 2D) displayed a better tendency than that in "Before" conformation (Figure 2C), indicating a better efficiency in "After" conformation. To further assess the degree of successful patterns, the pattern yield was also determined (Figure S16). The result illustrated that the pattern yield in the "After" conformation was higher than that in "Before" conformation. Note that when obtaining the pattern yield from the AFM images, the patterned origami could be counted as long as we could recognize the digits (Figure S6-S15).

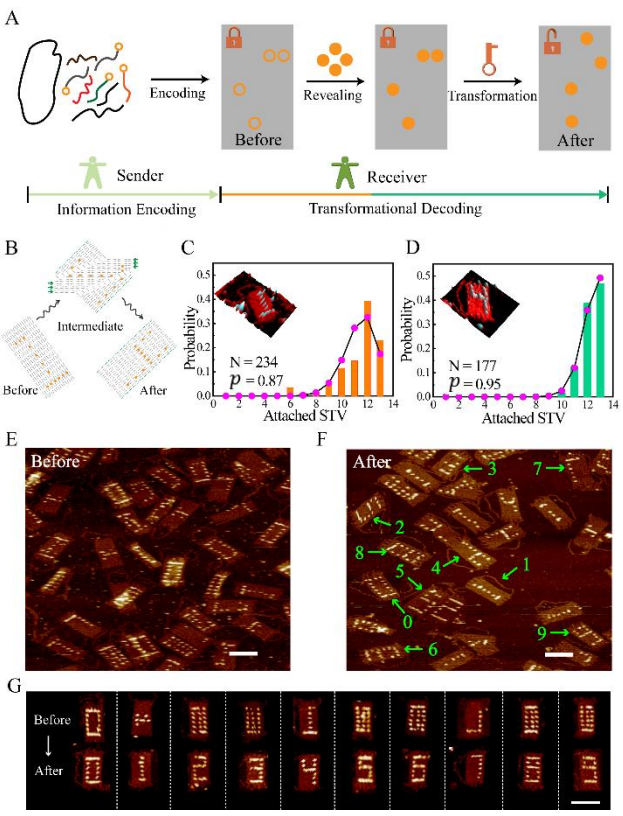

Figure 2. The patterns transfer in reconfigurable DODA. (A). Schematic of reconfigurable DODA as the hiding medium for steganography. The whole

process consisted of information coding and transformational decoding. (B). Schematic of reconfigurable DODA with 6 × 6 lattice (36 attachment sites) for transferring pattern of digit "4". (C-D). Histograms (bars) and calculated binomial distributions (lines) for the number of attached STV for DODA in "Before" (C) and "After" (D) conformation (digit "4" as an example). The insets were 3D AFM images of the digit "4" in "Before" (left) and "After" (right) conformation. N, the exact number of well-defined DODA. p, the average attachment probabilities, used to generate the calculated binomial distributions are indicated for each case. (E). AFM image of the complex sample containing all 0-9 digits in "Before" and "After" conformation (F). (G). High magnification AFM images of ten reconfigurable DODA displaying 0-9 digits transformed from "Before" to "After" conformation. Scale bars, 100 nm.

When all the ten patterned samples were mixed, it was difficult to identify the individual digits in the "Before" conformation (Figure 3E), while it was much easier to identify all the digits as soon as possible when the DODAs were transformed to the "After" conformation (Figure 3F). It is worth noting that the DODAs can be adsorbed on mica surface with the patterns facing up or facing down, and the scaffolded loops served as the markers for distinguishing mirror patterns (e.g. 2 and 5, 6 and 9). When a DODA lands on mica with its pattern facing up, the scaffolded loop appeared on its left side. If the scaffolded loop was observed on the right side of a DODA, the origami was adsorbed on mica upside down (Figure S17). These results all illustrated that the transformation of the DODA from "Before" to "After" successfully realized the patterns transfer, and helped to identify the informational patterns. (Table S4). Seen another way, if the information in the DODA was not simple patterns, but some important messages invisible to naked eye, it would be an ingenious way to do some cryptographic algorithms to deliver important information.

Having demonstrated the feasibility for steganography strategy in reconfigurable DODA, we then explored its further application in cryptographic algorithm for information security. In our everyday lives, important information is usually coded before transmission and then decoded to reveal the original information to protect the privacy of the communications. From the application point of view, the fact that important information after decoding pellucid to the public can clearly limit feasible applications. In some cases, for example, only the receiver would want to know the results without sharing with the public. Therefore, some cryptographic algorithms such as Morse code and American Standard Code for Information Interchange (ASCII) would be needed to provide as a protection for completely secretive MIC. Here we used the popular and simple ASCII as the cryptographic algorithm. Figure 3A illustrated the cryptography in reconfigurable DODA. Without the cryptographic algorithm ASCII, even the information was decoded with the aid of transformation, the information was still something intuitively random, meaningless and unintelligible for attackers. Only the proper receiver who kept the cryptographic algorithm ASCII could reveal the original information. In other words, the encoded information cannot be read until after both the conformation transformation and ASCII cracking processes (Figure 3A). Additionally, the conformation transformation conditions and codes cracking algorithm are unknown to the public and only accessible to the authorized party, suggesting greatly enhanced information security of the reconfigurable DODA hiding medium.

To test the feasibility of this idea, we created ACSII barcodes to realize the secret communication between the sender and receiver. Following the STV attachment (represent binar '1's) and no STV attachment (binary '0's) that made up ASCII (Figure S18 and Table S5), we constructed barcodes including digicipher and complex messages in reconfigurable DODA. To construct such barcodes, it was crucial to understand the reading rules of binary-coded DODA firstly. As shown in Figure S19, the four STV attachment sites (black ones) on top left of DODA were the starting marker for reading. Just like barcodes, each spot in the pattern represented a distinct digit of the binary numbers encoding the information. The ASCII values were read along the length of the DODA and the final codes were read along the width. Then we selected the 4×4 lattice and 5×5 lattice to construct barcodes. Interestingly, during the decoding process, we found there were two modules. One was if the STV attachment sites were central symmetry, the coded and decoded message kept the same. Otherwise if the STV attachment sites were not central symmetry, the coded and decoded message were different in the two different conformations. To be more specific, taken the 4×4 lattice which could be regarded as a 4×4 matrix (Figure S20A), as an example, each STV attachment site represented as a_{ij}, (i, j = 1,2,3,4) When the STV attachment sites were central symmetry (as long as satisfied the equation $\sum_{k=1}^{n}(i_k + j_k) = 5n\ (n = 2,4,6\ldots)$, the digicipher in the reconfigurable DODA kept the same after decoding. Two examples were given (1248-1248, 8421-8421, Figure S20B and Figure S21-22) to verify this module. For the other module, four examples were given (0192-2016, 0193-2017, 1082-2018, 1083-2019, Figure 3B and Figure S23-26).

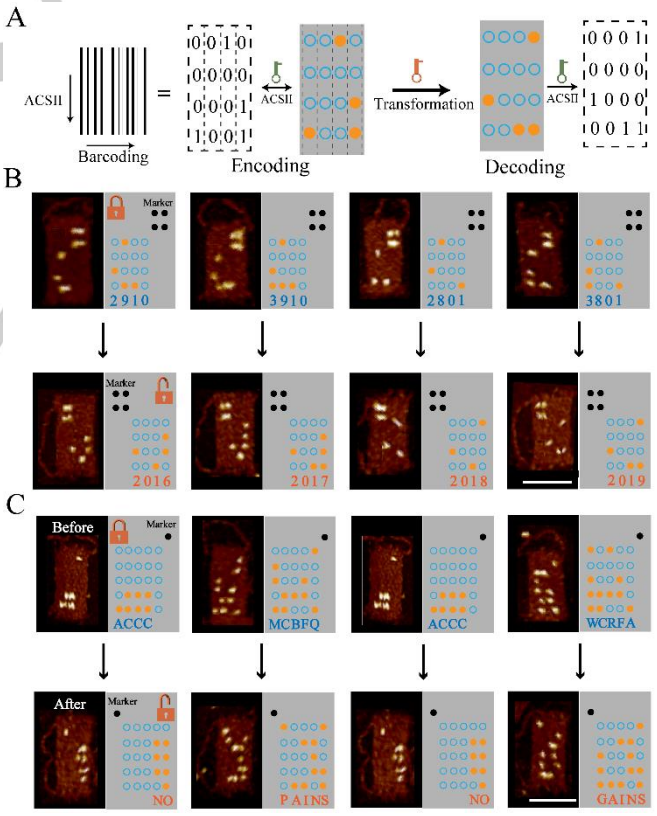

Figure 3. An illustration of the barcodes in reconfigurable DODA. (A). Schematic of reconfigurable DODA with 4×4 lattice for coding and decoding barcodes. The whole process consisted of information coding and information decoding. The information in the DODA can be regarded as barcodes. The ASCII value was read along the length of the DODA, and the barcodes was obtained along the width of the DODA. The public key was the ASCII, which helped to encode and decode the information. The private key is the transformation, which helped to decode the information. (B). The designed

10.1002/anie.202003823

barcodes for special years (2016-2019) were different in the two different conformations. (C). AFM images of DNA origami in "Before" conformation displaying coded messages "CCCA, QFBCM, CCCA, AFRS" (up ones) and decoded messages "NO PAINS NO GAINS" after transformation (bottom ones). Scale bars, 100 nm.

To transfer more complex message, a 5×5 lattice was then selected (Figure S27). As the basic principle of digicipher described above, if we wanted to transmit important message such as "NO PAINS NO GAINS", the original message was encoded into ciphertext "CCCA, QFBCM, CCCA, AFRCW" in "Before" conformational DODA, and then decoded it into "NO PAINS NO GAINS" with the transformation key and ASCII key (Figure 3C, Figure S28-30).

In order to enhance encoding complexity and security, a more sophisticated two-step anti-counterfeiting approach was further demonstrated. As shown in Figure 4A, after the decoding by the conformational transformation, the encoded information needs to be further decoded by the second step of information recovery, which was realized by toehold-medicated strand displacement reactions. The detailed scheme was described in Figure 4B-C. The DNA strand T3 was blocked with T1 and T2 initially (the complex formed by T1, T2, T3 was called an "inhibited DNA assembly"; Figure 4C). After the conformational transformation bringing the inhibited DNA assembly to close proximity of strand T4 (from 17.7 nm before the transformation to 5 nm after the transformation) and the subsequent addition of the second decoding key, the inhibited DNA assembly was activated and the DNA strand T3 bound to the T4 strands via a toehold-mediated strand displacement reaction, which made the T2 strand available for the subsequent hybridization with biotin-labeled T5 strand for the visualization of the recovered final information. To further demonstrate the versatility of this new method, we designed and demonstrated the coding and decoding of "S-J-T-U" patterns by using the anti-counterfeiting scheme (Figure 4D, Figure S31-S46).

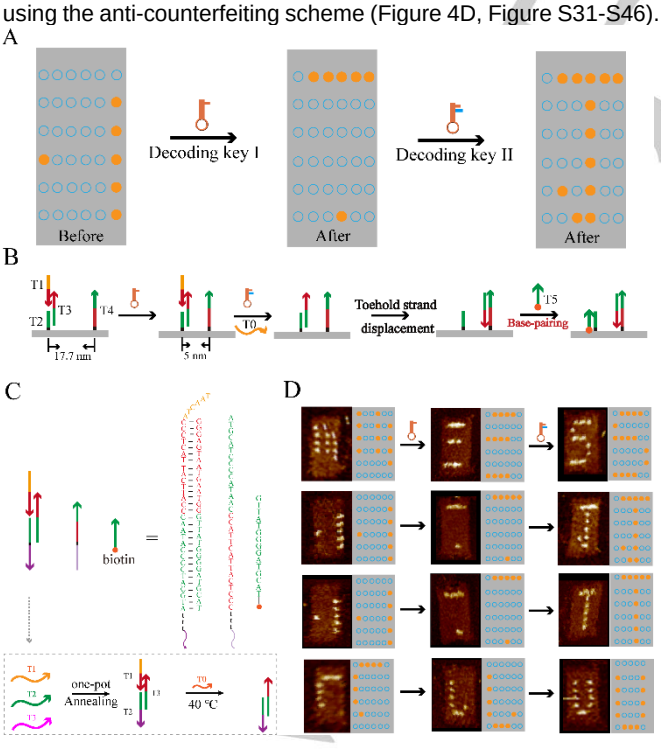

Figure 4. Schematic of anti-counterfeiting MIC in DODA. (A) The anti-counterfeiting MIC is decoded with two sets of keys. (B) The detailed scheme of the decoding process of the anti-counterfeiting MIC. (C) The sequences of the inhibited DNA assembly (T1, T2, T3), T4 foothold, and biotin-labeled strand. The inset showed the assembly of the inhibited DNA assembly and its activation by the second key (T0). (D) AFM images and schematic diagrams showing before-decoding and after-decoding origami arrays with hidden information of "SJTU".

Firstly, the original patterns "S-J-T-U" was encoded into cipher patterns " ㅐ-ㅣ-ㅜ-ㄱ " in the "Before" DODAs. To decode, the patterns were changed to " ㅡ-ㅜ-ㅜ-ㄴ " with the addition of the first transformation key. At this time, the patterns were only partially revealed, and can carry intentionally designed decoy information. The actual "S-J-T-U". patterns were revealed by the addition of the second decoding DNA key. The decoding yields were 38.5%, 35.9%, 29.1% and 40.4% for the patterns of "S", "J", "T", and "U", respectively (Table S7-S10). This non-reversible information recovering process also provides an anti-counterfeiting mechanism: Even if skilled counterfeiters decoded the information, the intended receiver can verify the authenticity of information and whether it has been compromised.

Conclusion

Overall, the reconfigurable DODA provides an excellent encoding substrate for secured information storage, transfer, and recovery. The efficiency of the DODA transformation from "Before" to "After" conformation is as high as 93.2%, providing a solid foundation for its applications in MIC. At the same time, some of the main challenges in MIC, such as duplication, high data storage density, and anti-counterfeiting, can also be addressed by using the highly adaptable reconfigurable DODA. Along with advantage of high data storage density in those the bare DNA origami [20] (offers density of up to 10^{18} bytes per mm^3), the modification of their staple strands allows more complex of data formats to be tailored. For anti-counterfeiting, the two-step decoding scheme of MIC provides additional safety for storing information in DODAs. Overall three key anti-counterfeiting features in DODAs improve the cryptographic security: 1) The geometry of the DODAs remains the same before and after the transformation; 2) A unique cryptographic algorithm (e.g. with ASCII) can be used to code and decode the information; 3) Two sets of orthogonal DNA keys are required to transfer the DODAs, and to recover the information via toehold-medicated strand displacement reactions. DNA nanostructures (e.g. DNA origami and SST structures) of larger sizes can be further used to extend the data storage capacity. Larger DNA origami can be designed by the using of long scaffolds [21], hierarchical assembly of DNA origami [22], surface-assisted large-scale assembly of DNA origami. [23], and base-stacking hierarchical assembly[24], etc. Alternatively, SST (DNA bricks) allows the assembly of prescribed nanostructures without size limitation caused by DNA scaffolds [25].

Despite the application in information security, the reconfigurable DODA can also be used in other fields such by assembly of different functional nanomaterials. For example, in molecular biology field, it can be utilized as a platform to analyze and control biomolecular interactions[26] (e.g., enzymatic reactions, chemical reactions, fluorescence resonance energy transfer, etc) at a single-molecule level, especially allows novel biological experiments aimed at modelling complex protein assemblies and

examining the effects of spatial organization. This will hold a great potential to complete more complex and difficult tasks for clinic diagnostics and bioanalytical applications.

Acknowledgements

The authors are grateful for the financial support from the National Natural Science Foundation of China (Nos. 81822024, 11761141006), the Natural Science Foundation of Shanghai, China (Nos. 19520714100, 19ZR1475800), the National Key Research and Development Program of China (Grant No. 2017YFC1200904), and the Project of Shanghai Jiao Tong University (2019QYA03 and YG2017ZD07).

Keywords: Reconfigurable DNA Origami Domino Array (DODA) • Molecular Information Coding (MIC) • Steganography and Cryptography

[1] N. C. Seeman, H. F. Sleiman, *Nat. Rev. Mater.* **2017**, *3*.
[2] P. W. K. Rothemund, *Nature* **2006**, *440*, 297.
[3] aY. Tian, T. Wang, W. Liu, H. L. Xin, H. Li, Y. Ke, W. M. Shih, O. Gang, *Nat. Nanotechnol.* **2015**, *10*, 637-644; bW. Liu, J. Halverson, Y. Tian, A. V. Tkachenko, O. Gang, *Nat. Chem.* **2016**, *8*, 867-873; cR. Schreiber, J. Do, E. M. Roller, T. Zhang, V. J. Schuller, P. C. Nickels, J. Feldmann, T. Liedl, *Nat. Nanotechnol.* **2014**, *9*, 74-78; dF. Hong, F. Zhang, Y. Liu, H. Yan, *Chem. Rev.* **2017**, *117*, 12584-12640.
[4] aS. Rinker, Y. G. Ke, Y. Liu, R. Chhabra, H. Yan, *Nat. Nanotechnol.* **2008**, *3*, 418-422; bN. V. Voigt, T. Torring, A. Rotaru, M. F. Jacobsen, J. B. Ravnsbaek, R. Subramani, W. Mamdouh, J. Kjems, A. Mokhir, F. Besenbacher, K. V. Gothelf, *Nat. Nanotechnol.* **2010**, *5*, 200-203; cN. Y. Wong, H. Xing, L. H. Tan, Y. Lu, *J. Am. Chem. Soc.* **2013**, *135*, 2931-2934.
[5] aA. Gopinath, E. Miyazono, A. Faraon, P. W. K. Rothemund, *Nature* **2016**, *535*, 401-405; bR. Jungmann, M. S. Avendaño, J. B. Woehrstein, M. Dai, W. M. Shih, P. Yin, *Nat. Methods* **2014**, *11*, 313-321; cG. P. Acuna, F. M. Moller, P. Holzmeister, S. Beater, B. Lalkens, P. Tinnefeld, *Science* **2012**, *338*, 506-510; dP. Wang, T. A. Meyer, V. Pan, P. K. Dutta, Y. Ke, *Chem* **2017**, *2*, 359-382.
[6] aH. Bui, C. Onodera, C. Kidwell, Y. P. Tan, E. Graugnard, W. Kuang, J. Lee, W. B. Knowlton, B. Yurke, W. L. Hughes, *Nano Lett.* **2010**, *10*, 3367-3372; bG. Tikhomirov, P. Petersen, L. Qian, *Nat. Nanotechnol.* **2016**, *12*, 251-260; cG. Tikhomirov, P. Petersen, L. Qian, *Nature* **2017**, *552*, 67; dJ. B. Knudsen, L. Liu, A. L. B. Kodal, M. Madsen, Q. Li, J. Song, J. B. Woehrstein, S. F. Wickham, M. T. Strauss, F. Schueder, J. Vinther, A. Krissanaprasit, D. Gudnason, A. A. A. Smith, R. Ogaki, A. N. Zelikin, F. Besenbacher, V. Birkedal, P. Yin, W. M. Shih, R. Jungmann, M. D. Dong, K. V. Gothelf, *Nat. Nanotechnol.* **2015**, *10*, 892-898; eS. Fan, D. Wang, A. Kenaan, J. Cheng, D. Cui, J. Song, *Small* **2019**, *15*, e1805554; fX. Liu, F. Zhang, X. Jing, M. Pan, P. Liu, W. Li, B. Zhu, J. Li, H. Chen, L. Wang, J. Lin, Y. Liu, D. Zhao, H. Yan, C. Fan, *Nature* **2018**, *559*, 593-598.
[7] M. J. Dai, R. Jungmann, P. Yin, *Nat. Nanotechnol.* **2016**, *11*, 798-807.
[8] Y. Zhang, F. Wang, J. Chao, M. Xie, H. Liu, M. Pan, E. Kopperger, X. Liu, Q. Li, J. Shi, L. Wang, J. Hu, L. Wang, F. C. Simmel, C. Fan, *Nat. Commun.* **2019**, *10*, 5469.
[9] Y. Zhang, V. Pan, X. Li, X. Yang, H. Li, P. Wang, Y. Ke, *Small* **2019**, *15*, e1900228.
[10] aY. G. Ke, T. Meyer, W. M. Shih, G. Bellot, *Nat. Commun.* **2016**, *7*, 10935; bL. Zhou, A. E. Marras, H. J. Su, C. E. Castro, *Nano Lett.* **2015**, *15*, 1815.
[11] aK. Lund, A. J. Manzo, N. Dabby, N. Michelotti, A. Johnson-Buck, J. Nangreave, S. Taylor, R. Pei, M. N. Stojanovic, N. G. Walter, E. Winfree, H. Yan, *Nature* **2010**, *465*, 206-210; bH. Z. Gu, J. Chao, S. J. Xiao, N. C. Seeman, *Nature* **2010**, *465*, 202-205; cA. J. Thubagere, W. Li, R. F. Johnson, Z. Chen, S. Doroudi, Y. L. Lee, G. Izatt, S. Wittman, N. Srinivas, D. Woods, E. Winfree, L. Qian, *Science* **2017**, *357*.
[12] aD. R. Han, S. Pal, Y. Liu, H. Yan, *Nat. Nanotechnol.* **2010**, *5*, 712-717; bF. Zhang, J. Nangreave, Y. Liu, H. Yan, *Nano Lett.* **2012**, *12*, 3290-3295.
[13] A. E. Marras, L. Zhou, H. J. Su, C. E. Castro, *Proc. Natl. Acad. Sci. U. S. A.* **2015**, *112*, 713-718.
[14] aN. Wu, I. Willner, *Nano Lett.* **2016**, *16*, 6650-6655; bA. Kuzyk, M. J. Urban, A. Idili, F. Ricci, N. Liu, *Sci. Adv.* **2017**, *3*, e1602803.
[15] aY. Yang, M. Endo, K. Hidaka, H. Sugiyama, *J. Am. Chem. Soc.* **2012**, *134*, 20645-20653; bA. Kuzyk, Y. G. Yang, X. Y. Duan, S. Stoll, A. O. Govorov, H. Sugiyama, M. Endo, N. Liu, *Nat. Commun.* **2016**, *7*, 10591.
[16] E. Kopperger, J. List, S. Madhira, F. Rothfischer, D. C. Lamb, F. C. Simmel, *Science* **2018**, *359*, 296.
[17] S. Lauback, K. R. Mattioli, A. E. Marras, M. Armstrong, T. P. Rudibaugh, R. Sooryakumar, C. E. Castro, *Nat. Commun.* **2018**, *9*, 1446.
[18] J. Song, Z. Li, P. F. Wang, T. Meyer, C. D. Mao, Y. G. Ke, *Science* **2017**, *357*.
[19] aS. M. Du, S. Zhang, N. C. Seeman, *Biochemistry* **1992**, *31*, 10955-10963; bD. F. Wang, J. Song, P. F. Wang, V. Pan, Y. W. Zhang, D. X. Cui, Y. G. Ke, *Nat. Protoc.* **2018**, *13*, 2312-2329.
[20] L. Ceze, J. Nivala, K. Strauss, *Nat. Rev. Genet.* **2019**, *20*, 456-466.
[21] aH. Zhang, J. Chao, D. Pan, H. Liu, Q. Huang, C. Fan, *Chem. Commun.* **2012**, *48*, 6405-6407; bA. Marchi, N, I. Saaem, B. Vogen, N, S. Brown, T. LaBean, H, *Nano Lett.* **2014**, *14*, 5740-5747.
[22] aW. Pfeifer, B. Saccà, *ChemBioChem* **2016**, *17*, 1063-1080; bZ. Li, M. Liu, L. Wang, J. Nangreave, H. Yan, Y. Liu, *J. Am. Chem. Soc.* **2010**, *132*, 13545-13552; cT. Tigges, T. Heuser, R. Tiwari, A. Walther, *Nano Lett.* **2016**, *16*, 7870-7874; dW. Liu, H. Zhong, R. Wang, N. C. Seeman, *Angew. Chem., Int. Ed.* **2011**, *123*, 264-267; eR. Jungmann, M. Scheible, A. Kuzyk, G. Pardatscher, C. E. Castro, F. C. Simmel, *Nanotechnology* **2011**, *22*, 275301; fW. Pfeifer, P. Lill, C. Gatsogiannis, B. Saccà, *ACS Nano* **2018**, *12*, 44-55; gY. Yang, D. Han, J. Nangreave, Y. Liu, H. Yan, *Acs Nano* **2012**, *6*, 8209-8215.
[23] aA. A. Rafat, T. Pirzer, M. B. Scheible, A. Kostina, F. C. Simmel, *Angew. Chem., Int. Ed.* **2014**, *53*, 7665-7668; bS. Woo, P. W. Rothemund, *Nat. Commun.* **2014**, *5*, 4889-4898; cY. Suzuki, M. Endo, H. Sugiyama, *Nat. Commun.* **2015**, *6*, 8052; dC. Kielar, S. Ramakrishnan, S. Fricke, G. Grundmeier, A. Keller, *ACS Appl. Mater. Interfaces* **2018**, *10*, 44844-44853; eS. Kocabey, S. Kempter, J. List, Y. Xing, W. Bae, D. Schiffels, W. M. Shih, F. C. Simmel, T. Liedl, *Acs Nano* **2015**, *9*, 3530-3539; fY. Suzuki, H. Sugiyama, M. Endo, *Angew. Chem., Int. Ed.* **2018**, *57*, 7061-7065.
[24] aS. Woo, P. W. K. Rothemund, *Nat. Chem.* **2011**, *3*, 620-627; bT. Gerling, K. F. Wagenbauer, A. M. Neuner, H. Dietz, *Science* **2015**, *347*, 1446-1452; cA. Rajendran, M. Endo, Y. Katsuda, K. Hidaka, H. Sugiyama, *Acs Nano* **2011**, *5*, 665-671.
[25] aL. L. Ong, N. Hanikel, O. K. Yaghi, C. Grun, M. T. Strauss, P. Bron, J. Lai-Kee-Him, F. Schueder, B. Wang, P. Wang, J. Y. Kishi, C. Myhrvold, A. Zhu, R. Jungmann, G. Bellot, Y. Ke, P. Yin, *Nature* **2017**, *552*, 72-77; bZ. Zhang, J. Song, F. Besenbacher, M. Dong, K. V. Gothelf, *Angew. Chem., Int. Ed.* **2013**, *52*, 9389-9393; cY. G. Ke, L. L. Ong, W. Sun, J. Song, M. D. Dong, W. M. Shih, P. Yin, *Nat. Chem.* **2014**, *6*, 994-1002.
[26] aP. C. Nickels, B. Wunsch, P. Holzmeister, W. Bae, L. M. Kneer, D. Grohmann, P. Tinnefeld, T. Liedl, *Science* **2016**, *354*, 305-307; bY. Ke, S. Lindsay, Y. Chang, Y. Liu, H. Yan, *Science* **2008**, *319*, 180-183; cF. Kilchherr, C. Wachauf, B. Pelz, M. Rief, M. Zacharias, H. Dietz, *Science* **2016**, *353*, aaf5508-aaf5508; dG. Grossi, M. D. E. Jepsen, J. Kjems, E. S. Andersen, *Nat. Commun.* **2017**, *8*, 992.

10.1002/anie.202003823

Entry for the Table of Contents

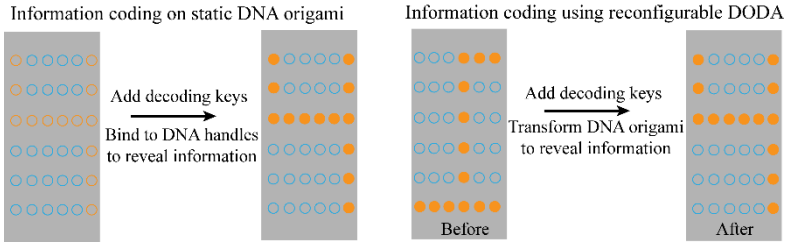

We demonstrated a novel steganography and cryptography molecular information coding strategy in a reconfigurable DNA origami domino array (DODA) synchronously. This strategy opens new opportunities for high-density information storage as well as information security against decoding, duplication and forgery, overcoming the key difficulties in MIC technologies.